

Electronic reconstruction at $\text{SrMnO}_3 - \text{LaMnO}_3$ superlattice interfaces

Șerban Smadici,¹ Peter Abbamonte,¹ Anand Bhattacharya,² Xiaofang Zhai,¹
Andrivo Rusydi,³ James N. Eckstein,¹ Samuel D. Bader,² and Jian-Min Zuo¹

¹*Frederick Seitz Materials Research Laboratory, University of Illinois, Urbana, Illinois 61801, USA*

²*Center for Nanoscale Materials and Materials Science Division,
Argonne National Laboratory, Illinois 60439, USA*

³*Institute of Applied Physics, University of Hamburg, D-20355, Germany*

We use resonant soft x-ray scattering to study electronic reconstruction at the interface between the Mott insulator LaMnO_3 and the “band” insulator SrMnO_3 . Superlattices of these two insulators were shown previously to have both ferromagnetism and metallic tendencies [Koida *et al.*, Phys. Rev. B **66**, 144418 (2002)]. By studying a judiciously chosen superlattice reflection we show that the interface density of states exhibits a pronounced peak at the Fermi level, similar to that predicted by Okamoto *et al.* [Phys. Rev. B **70**, 241104(R) (2004)]. The intensity of this peak correlates with the conductivity and magnetization, suggesting it is the driver of metallic behavior. Our study demonstrates a general strategy for using RSXS to probe the electronic properties of heterostructure interfaces.

PACS numbers: 71.45.Gm, 74.25.Jb, 78.70.Ck

The interface between two correlated electron systems may have properties that are qualitatively different from either of the two constituents, providing a potential route to new devices and physical properties. [1] An example is the interface between the d^1 Mott insulator LaTiO_3 (LTO) and the d^0 band insulator SrTiO_3 (STO), which experiments on superlattice heterostructures have suggested is metallic [2]. Dynamical mean field theory (DMFT) studies of this interface have suggested that the metallic behavior is driven by interfacial electronic reconstruction, characterized by the appearance of a quasiparticle peak at the Fermi level in the density of states of the interface layer [3, 4]. Efforts to find this peak with angle-integrated photoemission studies of LTO-STO superlattices observed a small Fermi surface crossing [5]. However, a peak in the density of states clearly associated with the buried interface has not yet been observed.

Another example of a Mott insulator - band insulator interface is $\text{LaMnO}_3 - \text{SrMnO}_3$. LaMnO_3 (LMO) is a Mott insulator with a $t_{2g}^3 e_g^1$ configuration while SrMnO_3 (SMO), which has a $t_{2g}^3 e_g^0$ configuration, can be considered a high-spin band insulator because its e_g shell is empty. Therefore, apart from the presence of the core t_{2g} spins, LMO-SMO is analogous to the LTO-STO system. A recent DMFT calculation predicted that the LMO-SMO interface should be a ferromagnetic metal, governed by double-exchange hopping of the e_g electrons. [6] Large period LMO-SMO heterostructures synthesized previously were shown to have both ferromagnetism and metallic tendencies [7], however it is not clear whether this derives from electronic reconstruction at the interfaces.

In this Letter we present a study of LMO-SMO superlattices with resonant soft x-ray scattering (RSXS). By judiciously choosing the thicknesses of the LMO and SMO sublayers, we obtained a structure whose third or-

der superlattice reflection is directly sensitive to the density of states (DOS) of the interface MnO_2 layer. We show that the DOS of the interface layer exhibits a pronounced quasiparticle resonance at E_F whose intensity correlates with the magnetization and conductivity of the overall structure. Our results confirm the predictions of Ref. [3, 4] and demonstrate a general strategy for using RSXS to study the electronic structure of heterostructure interfaces.

Superlattices consisting of seven periods of $(8 \times \text{LMO} + 4 \times \text{SMO})$ and six periods of $(10 \times \text{LMO} + 5 \times \text{SMO})$ layers were grown on SrTiO_3 (STO) substrates by molecular beam epitaxy. The samples will be denoted $(\text{LMO})2n/(\text{SMO})n$ with $n = 4$ or $n = 5$ in the following. In order to avoid oxygen vacancies, which can cause anomalous metallic behavior through electron doping [8, 9], the samples were both grown and post-annealed in flowing ozone. Large amplitude RHEED oscillations indicated two-dimensional epitaxial growth and STEM images showed well-defined superlattice interfaces (Fig. 1b). The SMO and LMO overlayers in these structures are under +2.8% and -2.1% strain, respectively, which likely alters the exact pattern of orbital and magnetic order in the sublayers, but will not by itself induce metallic behavior [10, 11]. X-ray reflectivity measurements showed clear interference fringes (Fig. 1a), indicating flat interfaces over macroscopic distances.

RSXS measurements were carried out at the soft x-ray undulator beamline X1B at the National Synchrotron Light Source in a 10-axis UHV diffractometer [12, 13]. Measurements were done in specular geometry, i.e. with the momentum transfer perpendicular to the plane of the heterostructure. In this article momenta will be denoted in reciprocal units of the superlattice, i.e. Miller index L corresponds to a momentum $Q = 2\pi L/d$, where d is the repeat period of the structure. The incident light was

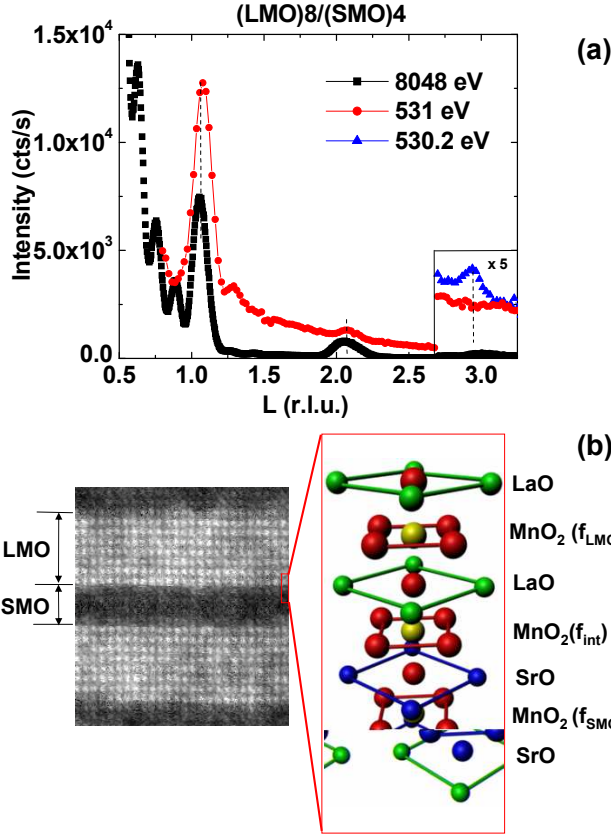


FIG. 1: (a) Specular x-ray scattering from the $n = 4$ superlattice with non-resonant hard x-rays (black circles), non-resonant soft x-rays (red circles), and soft x-rays tuned close to the Fermi energy (blue circles). Data are plotted on a linear scale to emphasize height differences between the peaks. (b) (left) STEM image of the $n = 4$ structure and (right) a drawing showing the interface region with scattering factors defined for the various atomic planes.

polarized in the scattering plane (π polarization) with the channeltron detector integrating over both final polarizations, i.e. both the $\pi \rightarrow \sigma$ and $\pi \rightarrow \pi$ scattering channels. Bulk sensitive RSXS measurements were performed at the Mn $L_{3,2}$ edges as well as the O K edge, which probes the $3d$ levels through hybridization, with the incident bandwidth set to 0.2 eV resolution. X-ray absorption (XAS) measurements were done *in situ* in total electron yield (TEY) mode and probed the top layer of the sample surface.

Prior to RSXS studies the superlattices were characterized with XAS, resistivity, magnetization, hard x-ray diffraction, and scanning transmission electron microscopy (STEM). XAS probes only the near-surface region which in the current case is the top LMO layer. The spectra (Figs. 3b and 4a; note the location of the Fermi energy) closely resemble past studies of LMO powders [14] indicating good surface quality. The resistivity of both samples exhibits a crossover to metallic behavior below $T_c \sim 225$ K (Fig. 2a and Ref. [15]). At this

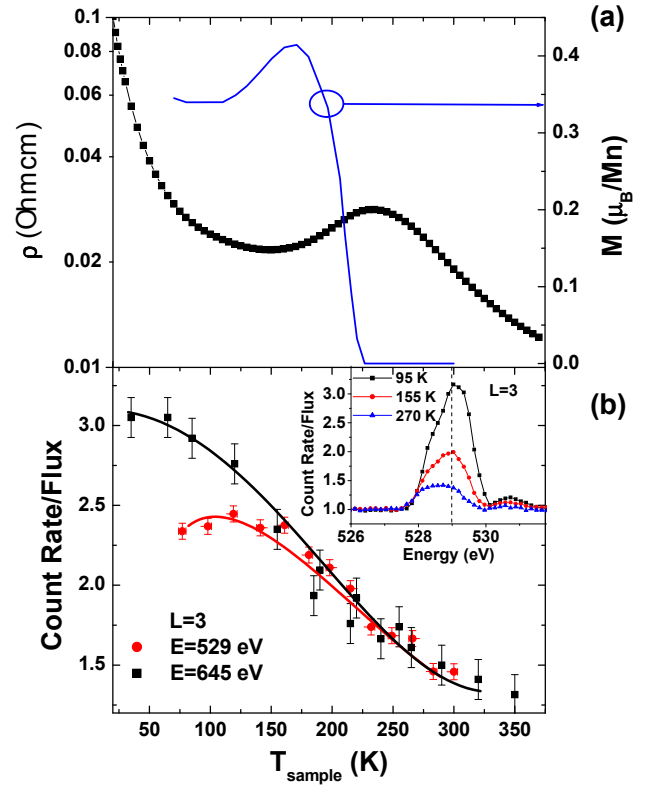


FIG. 2: (a). Temperature dependence of the conductivity and magnetization of the $n = 4$ structure when cooled in 50 G magnetic field. [15] (b). Temperature dependence of the $L = 3$ reflection at O K and Mn L_3 edges and $L = 3$ for the $n = 4$ sample. The inset shows temperature dependent scans at O K edge. Two quasiparticle peaks at the O K onset can be resolved.

temperature ferromagnetism also appears, with an average saturation magnetic moment at low temperatures of $1.75 \mu_B/\text{Mn}$ and $1.4 \mu_B/\text{Mn}$ for $n = 4$ and $n = 5$ samples, respectively. This behavior is consistent with double-exchange ferromagnetism as observed in previous studies [7, 15]. Because both of the constituents LMO and SMO are insulating and antiferromagnetic (A type and G type respectively) it seems likely, though this has not been proven, that magnetism originates at the interfaces.

In Fig. 1 we show hard x-ray diffraction data for the $n = 4$ superlattice. Thickness oscillations are visible, as well as several superlattice reflections residing at integer values of the Miller index L . A key observation is that the $L = 3$ reflection is suppressed. This is expected by symmetry. For a superlattice with sublayer thicknesses m and n the structure factor will vanish for any reflection $L = u + v$ where u/v is the fully reduced fraction of m/n . For the specific case of the $n = 4$ superlattice the structure factor for the $L = 3$ reflection is:

$$S(L = 3) = 2f_{\text{int}} - f_{\text{LMO}} - f_{\text{SMO}}, \quad (1)$$

where f_{LMO} and f_{SMO} are the scattering factors of the MnO_2 planes of the LMO and SMO layers, respectively, and f_{int} is the scattering factor for the MnO_2 plane at the interface (Fig. 1) [16]. Notice that the form factors for the LaO and SrO layers do not enter this quantity. The $L = 3$ reflection is forbidden by symmetry as long as the interface MnO_2 form factor is the average of the form factors of MnO_2 planes of the LMO and SMO layers. The intensity of this reflection is therefore a measure of the degree to which the mirror symmetry of the interface is broken. That this reflection is observed to be weak in hard x-ray diffraction measurements is an indication that the interfaces are sharp, with the symmetric form of Eq. 1 not disrupted by interdiffusion or other interface reconstruction.

Results of resonant scattering studies, which probe the unoccupied density of states, reveal something surprising (Fig. 1a). If the photon energy is tuned above the O K threshold - to a nonresonant condition - an L scan reveals that the $L = 3$ is extinguished, in agreement with hard x-ray measurements. However if the energy is tuned at 530.2 eV, near the Fermi onset, the $L = 3$ becomes visible. Evidently the symmetry of the LMO-SMO interface, while preserved by the atomic lattice, is broken electronically near the Fermi energy. This is evidence that the interfaces are electronically reconstructed.

Our primary observation is the energy dependence of the $L = 3$ reflection near the O K edge, shown in Fig. 3. This figure, which compares the intensity of the $L = 3$ reflection to an XAS spectrum of the LMO top layer, shows which part of the unoccupied density of states is reconstructed. The $L = 3$ reflection has maximum intensity at the edge onset, where RSXS probes states at the Fermi level. In addition, several weaker peaks are visible at 531.5 eV and 534 eV which coincide roughly with the Mn $e_{g,\uparrow}$ and $e_{g,\downarrow}$ bulk bands of LMO. We conclude that electronic reconstruction of the LMO-SMO interface occurs primarily near E_F although higher-energy states might also participate.

We propose that the main resonance observed at 529 eV corresponds to the presence of a quasiparticle peak at E_F , as predicted for a Mott-band insulator interface [3]. A connection to the DMFT calculations for LTO-STO superlattices in Ref. [3] can be made by noting that, in the absence of non-resonant scattering and excitonic effects, $\text{Im}[f_{int}]$ is proportional to the interface spectral function $A_{int}(z = z_{int}, z = z_{int}; \omega)$. It was shown in Ref. [3] that $A_{int}(z = z_{int}, z = z_{int}; \omega)$ has a strong peak at the Fermi energy E_F as we observe here. A quantitative comparison including the features at higher energy would require a microscopic model of the superlattice combined with Kramers-Kronig analysis of the data. The features at higher energy might arise from mixing of high-energy degrees of freedom including crystal field and Jahn-Teller effects, the Hubbard interaction and the Hund's rule exchange interaction, which

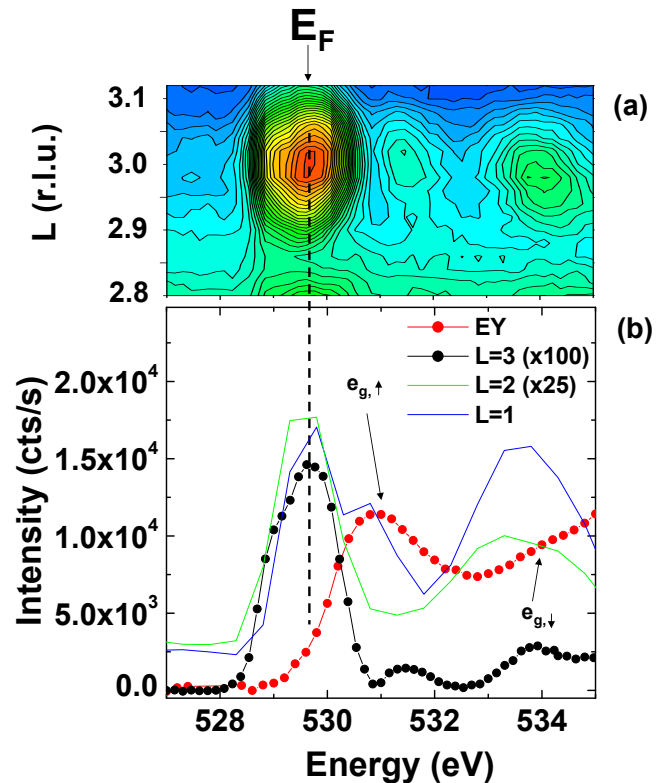


FIG. 3: (a). Resonance profile at $L = 3$ and O K edge for the $n = 4$ sample. The strongest resonance is at the energy of the doped holes and $L = 3$. (b). Scattering at $L = 3$ and $T = 90$ K (black), at $L = 1$ (blue) and $L = 2$ (green), compared to XAS data (red). The strong resonant enhancement before the O K edge is indicative of an electronic effect. The peaks at higher energy are aligned with features in the absorption spectra, as assigned in Ref. [14]. The peaks at 529 eV are interface states split-off from bulk bands.

require microscopic modeling beyond the scope of this article.

The connection between the $L = 3$ resonance at E_F and metallic behavior is also supported by its temperature dependence, shown in Fig. 2b. As the temperature is lowered the intensity of the E_F resonance rises, the inflection point coinciding with the peak in the resistivity and the onset of an in-plane magnetic moment [15] (Fig. 2a). This is evidence that the resonance is closely related to metallic behavior and that the magnetism and metallic conduction both arise from reconstruction of interfaces as considered by Okamoto *et al.* [3, 4]. Interestingly, the E_F peak also appears to be composed of two features separated by 0.75 eV with both peaks following a similar temperature dependence.

In order to study the magnetism of the superlattice, we also measured the $L = 3$ reflection at the Mn $L_{3,2}$ edges. Previous RSXS studies [17, 18, 19, 20, 21] of manganite systems have shown that both orbital and magnetic order can contribute to scattering at these edges. In our structures, in addition to magnetic order, one expects

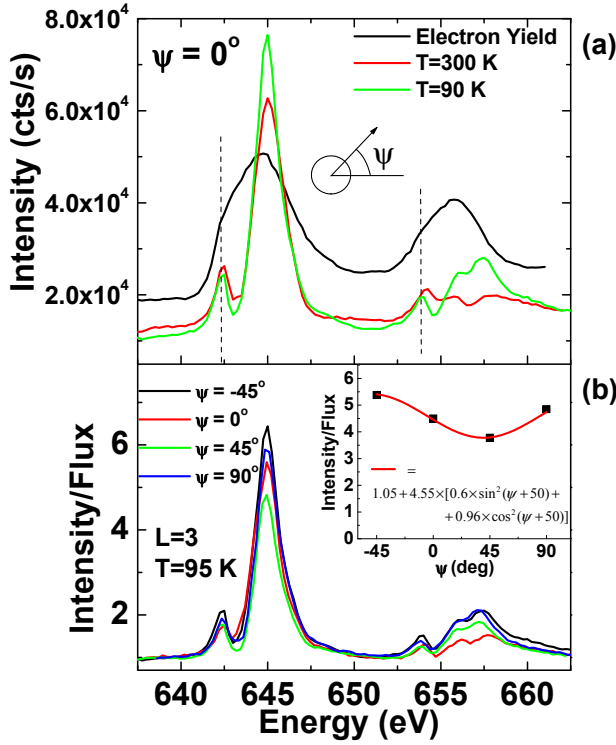


FIG. 4: (a). Energy profiles near Mn $L_{3,2}$ edges at $L = 3$ for two temperatures (red and green) and sample absorption measured by electron yield (black). In contrast to the L_3 edge, the L_2 edge resonance profile is strongly affected by the core hole. (b) $L = 3$ scattering at 645 eV for a few different azimuthal orientations. The inset shows the measured azimuthal dependence and a fit curve.

an interesting participation of the e_g orbital degree of freedom. In the SMO layer, which is under 2.8% tensile strain, the $d_{x^2-y^2}$ orbital should be lower in energy than the $d_{3z^2-r^2}$ orbital (z is along the c -axis). In LMO, which is under 2.1% compressive strain, the situation is reversed, which favors an occupied $d_{3z^2-r^2}$ orbital. One therefore expects the total structure to have a modulation in the orbital degree of freedom with the period of the superlattice. This is in addition to the Jahn-Teller effect that may still play a role in the LMO part of the superlattice despite the presence of strain. [10, 11] Separating charge, orbital and magnetic scattering at the Mn L edge through line shape analysis can be a cumbersome task. However, this can be done using the azimuthal dependence of the scattering. The magnetic scattering is proportional to $(\hat{\epsilon}_f^* \times \hat{\epsilon}_i) \cdot \mathbf{S}$, where $\hat{\epsilon}_i$ and $\hat{\epsilon}_f$ are the incident and final polarizations, respectively, and \mathbf{S} is the local spin. For our experimental geometry this simplifies to:

$$I \propto \cos^2(\theta) \sin^2(\psi) + \sin^2(2\theta) \cos^2(\psi), \quad (2)$$

where θ is the angle of incidence on the sample. In contrast, the strain-induced orbital scattering should be in-

dependent of ψ because strain does not break the tetragonal symmetry of the unit cell. Therefore, to make a rough estimate of the relative size of orbital and magnetic scattering, the $L = 3$ reflection was measured at a few values of the azimuthal angle ψ (Fig. 4). Good agreement is obtained between our measurements at four ψ angles and Eq. 2 (Fig. 4b, inset) with a magnetic moment at $\sim 50^\circ$ between the a and b axes and a constant offset equal to the off-resonance background. This suggests that the scattering is primarily magnetic in the present case.

Finally we discuss the temperature dependence at the Mn L edge (Fig. 2b), which agrees well with that observed at the O K edge. This again suggests that the E_F resonance and the interfacial superlattice magnetization are interrelated. The overall picture that emerges is that, as the temperature is lowered, ferromagnetism nucleates at interfaces increasing the metallic behavior and the spectral weight at E_F . The interfaces exhibit the same connection between charge carrier itineracy and magnetic order familiar from bulk colossal magnetoresistance materials.

In conclusion, we have used RSXS to investigate superlattices of the Mott insulator LaMnO_3 and the “band” insulator SrMnO_3 . By choosing a specific combination of superlattice reflection and layer periods we were able to isolate the electronic properties of the interface. We show that the interface density of states exhibits a pronounced peak at E_F as shown in the calculations of Okamoto *et al.* suggesting that ferromagnetism and metallic behavior in this system arise from electronic reconstruction of the interfaces. Our study demonstrates a general strategy for using RSXS to probe the electronic properties of interfaces.

The authors acknowledge helpful discussions with John Freeland and C.-C. Kao. This work was supported by the Office of Basic Energy Sciences at the U.S. Department of Energy. Resonant scattering experiments were supported under grant No. DE-FG02-06ER46285 and digital synthesis work under grant No. DE-AC02-06CH11357 sub-contract WO 4J-00181-0004A. Work at Argonne was supported under contract No. DE-AC02-06CH11357 and use of the NSLS under contract No. DE-AC02-98CH10886.

-
- [1] C. H. Ahn *et al.*, Rev. Mod. Phys. **78**, 1185 (2006).
 - [2] A. Ohtomo, D. A. Muller, J. L. Grazul, and H. Y. Hwang, Nature **419**, 378 (2002).
 - [3] S. Okamoto and A. J. Millis, Phys. Rev. B **70**, 241104(R) (2004).
 - [4] S. Okamoto and A. J. Millis, cond.-latt. 0507150 (2005).
 - [5] M. Takizawa *et al.*, Phys. Rev. Lett. **97**, 057601 (2006).
 - [6] C. Lin, S. Okamoto, and A. J. Millis, Phys. Rev. B **73**, 041104(R) (2006).
 - [7] T. Koida, M. Lippmaa, T. Fukumura, K. Itaka, Y. Matsumoto, M. Kawasaki, and H. Koinuma, Phys. Rev. B

- 66**, 144418 (2002).
- [8] G. Herranz *et al.*, arXiv:0704.2523.
 - [9] D. A. Muller, N. Nakagawa, A. Ohtomo, J. L. Gazul, and H. Y. Hwang, *Nature* **430**, 657 (2004).
 - [10] Y. Wakabayashi *et al.*, *Phys. Rev. Lett.* **96**, 017202 (2006).
 - [11] K. H. Ahn and A. J. Millis, *Phys. Rev. B* **64**, 115103 (2001).
 - [12] P. Abbamonte, L. Venema, A. Rusydi, I. Bozovic, G. Logvenov, and G. A. Sawatzky, *Science* **297**, 581 (2002).
 - [13] P. Abbamonte, A. Rusydi, Ş. Smadici, G. D. Gu, G. A. Sawatzky, and D. L. Feng, *Nature Physics* **1**, 155 (2005).
 - [14] M. Abbate *et al.*, *Phys. Rev. B* **46**, 4511 (1992).
 - [15] A. Bhattacharya *et al.*, *Appl. Phys. Lett.* **90**, 222503 (2007).
 - [16] The atomic scattering factors are tensors, i.e. $f = f^{i,j}$. For notational simplicity, however, we leave off the indices in our discussion.
 - [17] K. J. Thomas *et al.*, *Phys. Rev. Lett.* **92**, 237204 (2004).
 - [18] S. S. Dhesi *et al.*, *Phys. Rev. Lett.* **92**, 056403 (2004).
 - [19] S. B. Wilkins *et al.*, *J. Phys. Cond. Matt.* **18**, L323 (2006).
 - [20] U. Staub *et al.*, *Phys. Rev. B* **71**, 214421 (2005).
 - [21] J. Okamoto *et al.*, *Phys. Rev. Lett.* **98**, 157202 (2007).